ACS EARTH AND SPACE CHEMISTRY

Article

http://pubs.acs.org/journal/aesccq

Calcifying Response and Recovery Potential of the Brown Alga *Padina pavonica* under Ocean Acidification

David Iluz,[†] Simona Fermani,[‡] Michal Ramot,[†] Michela Reggi,[‡] Erik Caroselli,[§] Fiorella Prada,[§] Zvy Dubinsky,[†] Stefano Goffredo,[§] and Giuseppe Falini*[,‡]

[†]The Mina and Everard Goodman Faculty of Life Sciences, Bar-Ilan University, 52900 Ramat Gan, Israel

[‡]Department of Chemistry "Giacomo Ciamician", University of Bologna, Via Selmi 2, 40126 Bologna, Italy

[§]Marine Science Group, Department of Biological, Geological and Environmental Sciences, University of Bologna, Via Selmi 3, 40126 Bologna, Italy

Supporting Information

ABSTRACT: Anthropogenic carbon dioxide (CO_2) emissions are causing ocean acidification (OA), which affects calcifying organisms. Recent studies have shown that *Padina pavonica* investigated along a natural pCO_2 gradient seems to acclimate to OA by reducing calcified structures and changing mineralogy from aragonite to calcium sulfate salts. The aim of the present study was to study the potential for acclimation of *P. pavonica* to OA along the same gradient and in aquaria under controlled conditions. *P. pavonica* was cross-transplanted for 1 week from a normal pH site (mean values of pH_{TS} 8.1 and pCO_2 = 391 μatm) to a low pH site (mean values of pH_{TS} 7.4 and pCO_2 = 1044 μatm) and vice versa. Results showed that this calcifying alga did survive under acute environmental pH_{TS} changes but its calcification was significantly reduced. *P. pavonica* decalcified and changed mineralogy at pH_{TS} 7.4, but once brought back at pH_{TS} 8.1, it partially recovered the aragonite loss while preserving the calcium sulfate phases that formed under low pH_{TS}. These results suggest that *P. pavonica* could be used as a bioindicator for monitoring OA as well as localized anthropogenic acidity fluctuations.

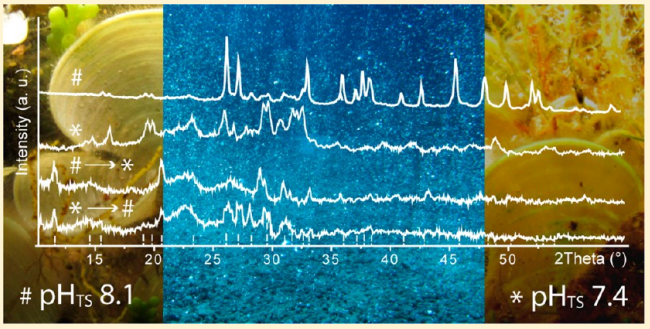

KEYWORDS: *algae, Padina pavonica, ocean acidification, transplanted, calcium carbonate, calcium sulfate phases*

INTRODUCTION

Atmospheric carbon dioxide (CO_2) has increased from 278 to 400 ppm since the dawn of the industrial period (1750−2017) and, concomitantly with the increase of other greenhouse gases, has driven a series of major environmental changes. The ocean acts as a climate integrator that, among other effects, captured 28% of anthropogenic CO_2 emissions, leading to ocean acidification (OA). Observations and models indicate that, since preindustrial times, the ocean average surface pH has declined by 0.1 units from the value of 8.2. In addition to a lower pH, the speciation of carbonate species is shifted, which results in a lower supersaturation with respect to calcium carbonate.[1,2]

Macroalgae are considered as indicators of marine environmental health as a result of their key role in the structuring and functioning of coastal ecosystems.[3,4] Their sessile habit and long life cycles make them long-term integrators of environmental change trends. The genus *Padina* (Dictyotales, Phaeophyceae), a brown calcified macroalga, is widely distributed in tropical and temperate coasts, such as the Macaronesian Islands, Mediterranean Sea, Caribbean Sea, Micronesia, and Polynesia.[5,6] In particular, *Padina pavonica* (Linnaeus) Thivy, 1960 plays a significant role as a dominant macrophyte in temperate oceans, being a conspicuous member of macroalgal communities in sub- and intertidal rocky shore systems.[7] *P. pavonica* is a worldwide distributed species of rocky shores of the sublittoral in tropical and temperate regions.[8] *P. pavonica* presents a biologically induced extracellular calcification, which results in whitish precipitations.[9−12] These carbonate deposits, predominantly aragonite needles, are arranged in concentric bands on both thallus surfaces,[13,14] with interspaces where reproductive structures, such as tetrasporangia, can develop. The side of the blade facing the sea surface with the enrolled margins represents the "upper" surface and is more calcified than the opposite side, the "lower" surface (Figure 1).[10,15]

Studies of the chlorophyte *Halimeda* have shown that calcification depends upon pH changes driven by photosynthesis.[16,17] Biochemical processes lead to acidic and alkaline zones and gradients on the thallus surface providing optimal microenvironments for calcification processes.[18] The pH range

Received: May 11, 2017
Revised: June 14, 2017
Accepted: June 20, 2017
Published: June 20, 2017

DOI: 10.1021/acsearthspacechem.7b00051
ACS Earth Space Chem. XXXX, XXX, XXX−XXX

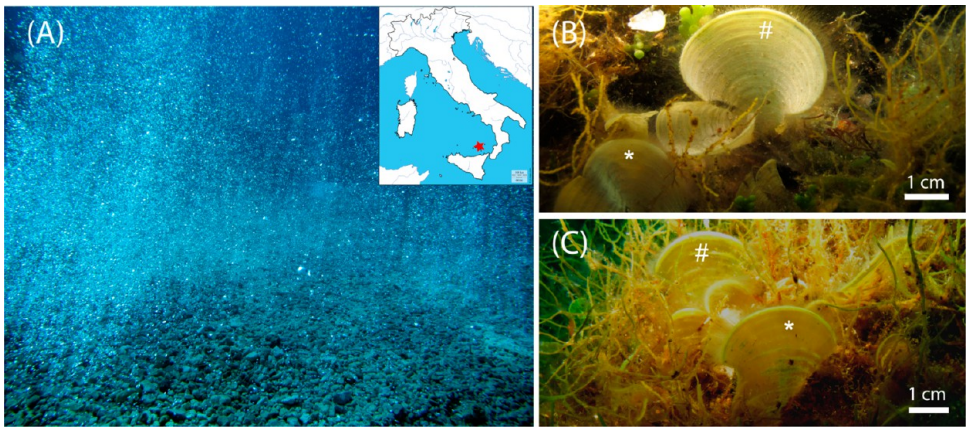

Figure 1. (A) Camera picture of the natural lab. The volcanic crater on the bottom of the ocean in proximity of Panarea Island (see red star on the map of Italy in the inset), where the CO_2 vent is localized. This site corresponds to Site 4, where the mean pH_{TS} is 7.4. The other site of study (Site 1) was at about 30 m from the crater, and there the mean pH_{TS} is 8.1. (B) Camera picture of the sample of *P. pavonica* at the Site 1. (C) Camera picture of the sample of *P. pavonica* at the Site 4. The thallus or body of *P. pavonica* forms fan-shaped clusters, in which the blade "upper" surface (#) and is more calcified than the opposite side, the "lower" surface (∗). The deposited minerals form concentric rings on the blades, which in the sample heavily calcified (B) appear fused, conferring to the blades a white color. In the sample low calcified (C), few white concerting rings are observable and the blades appear with a light brown color.

between 8.2 and 8.4 favors carbonate uptake via hydrogen carbonate and stabilizes the exchange system. A higher pH leads to a dramatic decline in photosynthetic rates and an increase in carbonate precipitation,[19] whereas under lower pH, carbonates start to dissolve. The effect of low pH/high pCO_2 on early life stages of *Phymatolithon lenormandii* (Areschoug) Adey was studied in a perturbation experiment. Among several parameters, calcification was monitored for 1 month under experimental conditions ranging from pH_{TS} 8.00 to 7.55. The results showed that calcification was still observed at the lowest pH, but for its maintenance, more energy was required.[20] In a similar study, Newcombe et al. showed that *Acetabularia acetabulum* algae could tolerate high CO_2 conditions (pCO_2 = 2283 μatm) but calcification was reduced and stem stiffness was decreased.[21]

Thus, calcifying algae are very sensitive to pH shifts. In *Padina* sp., extracellular calcification is arranged in concentric bands, as in Charophyceae, where it is attributed to different pH-based areas.[18] Protons from carbonate deposition sites (i.e., the alkaline bands) are transported and released in the non-calcifying areas of the thallus, the acidic bands, for hydrogen carbonate conversion. McConnaughey and Whelan assumed that protons generated by calcification mechanisms might support nutrient uptake.[22] The carbonate deposits function as a structure-strengthening skeleton and may act as a protection measure against grazers.[23,24] In a recent study, it was suggested that photosynthetic organisms could mitigate OA on a local scale. However, it was found that *P. pavonica*, which is resistant to acidification, does not prevent a reduction in the number of species of foraminifera.[25]

The genus *Padina* has been previously used to test OA effects.[10−12,26] *P. pavonica* investigated along a natural pCO_2 gradient off Panarea Island (Italy) seems to acclimate to OA by reducing the calcified regions and slightly altering their mineralogy from aragonite to calcium sulfate phases.[10] The aim of this study was to investigate *P. pavonica* calcifying response and recovery potential to OA in the field, along a natural pH gradient, and under controlled conditions in aquaria. The overarching hypothesis is that *P. pavonica* samples, which have been treated under OA conditions, are able to recover their calcifying potential at the normal pH conditions because *P. pavonica* calcifies through a biomineralization process that is induced by the biochemical activity of the organism[9,18] but is also affected by the living environmental conditions, as already shown.[10]

MATERIALS AND METHODS

Study Site. The sampling area is close to Panarea Island (Italy), an inactive volcano in the north of Sicily. Close to Panarea Island, there is an area delimited by the islets of Dattilo, Bottaro, Lisca Nera, and Lisca Bianca, characterized by a widespread presence of gas vents. In the main vent, a crater 20 × 14 m wide at the depth of ∼10 m generates a sustained column of bubbles from the seabed to the sea surface. In this crater, the stable CO_2 emission occurs without altering the seawater temperature and generates a pH gradient that extends for ∼30 m from the center of the crater to its periphery. Depth along the CO_2 gradient goes from 11.6 m at the crater to 9.2 m at the control site ∼34 m from the center of the crater. The distances and corresponding mean pH values are, for Site 1 control, d = 34 m and pH_{TS} 8.07 and, for Site 4, d = 3 m and pH_{TS} 7.40.

Sample Transplanting and Collection. Samples of *P. pavonica* were transplanted from ambient seawater (pH_{TS} 8.1) to acidified conditions (pH_{TS} 7.4) and vice versa during the month of June 2012. Along the Panarea pCO_2 gradient, native samples were transplanted for 1 week from Site 1 at pH_{TS} 8.1 to Site 4 at pH_{TS} 7.4 and vice versa. For aquaria experiments, the samples were placed immediately after collection in tanks with seawater from the corresponding stations.

Sample Incubation in Aquaria at Different pH Values. In the aquaria experiments, *P. pavonica* samples from Site 1 at pH_{TS} 8.1 were placed for 7 days at that same pH_{TS} and then for 7 days at pH_{TS} 7.4; conversely, samples collected at Site 4 were placed for 7 days at that same pH_{TS} and then for 7 days at pH_{TS} 8.1. One aquarium (300 L) was set at pH_{TS} 8.1, and another aquarium (300 L) was set at pH_{TS} 7.4. The aquaria lighting bulbs, filters, temperature, and pH were controlled with the AT Control System (Aqua Medic Company). In each aquarium, the salinity was 35 ppt (measured with a refractometer), the

DOI: 10.1021/acsearthspacechem.7b00051
ACS Earth Space Chem. XXXX, XXX, XXX−XXX

Table 1. Mineral Percentage (w/w) and Phase Composition of *P. pavonica* at Normal and Low pH Levels along a Natural pCO_2 Gradient and under Controlled Conditions in Aquaria[a]

	starting condition					transplanting condition					
			mineral phase composition (wt %)						mineral phase composition (wt %)		
	pH_{TS}	min c[b] (wt %)	A	C	CSp	pH_{TS}	treat[c] (days)	min c[b] (wt %)	A	C	CSp
natural lab	8.1	71 ± 3	97 ± 2	1.5 ± 0.9	1.0 ± 0.5	7.4	7	60 ± 4	21 ± 3	7 ± 4	72 ± 11
	7.4	61 ± 2	21 ± 5	4 ± 2	75 ± 11	8.1	7	66 ± 3	39 ± 4	4 ± 2	57 ± 6
aquaria	8.1	71 ± 3	97 ± 2	1.5 ± 0.9	1.0 ± 0.5	8.1[d]	7	72 ± 6	97 ± 3	1.5 ± 0.5	1.5 ± 1.0
	8.1[d]	72 ± 6	97 ± 3	1.5 ± 0.5	1.5 ± 1.0	7.4	7	60 ± 5	62 ± 7	1.0 ± 0.5	38 ± 5
	7.4	61 ± 2	21 ± 5	4 ± 2	75 ± 11	7.4[d]	7	62 ± 5	29 ± 9	2.0 ± 1.0	69 ± 10
	7.4[d]	63 ± 5	29 ± 9	2.0 ± 1.0	70 ± 10	8.1	7	67 ± 3	38 ± 5	2.0 ± 0.5	60 ± 10

[a]The samples collected from sites 1 and 4 were kept for 7 days at pH_{TS} 8.1 and 7.4 in aquaria for adaptation and then transplanted. A, C, and CSp indicate aragonite, magnesium calcite, and calcium sulfate phases, respectively. A mixture of calcium sulfate phases having a diverse hydration was detected, with the main calcium sulfate phases being gypsum, bassanite, and anhydrite. Uncertainties on the mineral content are standard deviations (n = 3), and those on mineral composition are associated to the Rietveld refinements. [b]min c indicates the mineral percentage in the algae. [c]treat indicates the treatment time at the transplanting conditions. [d]Samples kept in aquaria at the same pH_{TS} of the collection site for 7 days for adaptation.

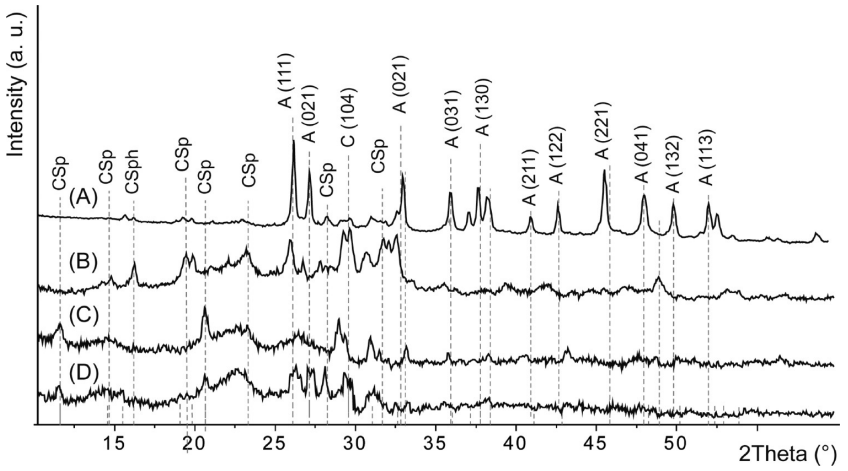

Figure 2. X-ray powder diffraction pattern of samples of *P. pavonica* cross-transplanted at the CO_2 vent: (A) sample collected in Site 1 at pH_{TS} 8.1, (B) sample collected in Site 4 at pH_{TS} 7.4, (C) sample collected in Site 1 at pH_{TS} 8.1 and transplanted to Site 4, and (D) sample collected in Site 4 at pH_{TS} 7.4 and transplanted to Site 1 at pH_{TS} 8.1. A, C, and CSp indicate aragonite, magnesium calcite, and calcium sulfate phases, respectively. The Miller indexes of aragonite diffraction peaks are indicated.

water temperature was 25 °C [controlled with a chiller, model TC20 (TECO)], and lighting lamps [metal halide (400 W)] were controlled by a controller (Advanced Control Lighting System, Sfiligoi Aquarium Lighting Company). The pH was measured with a pH sensor (on-line) controlled with the AT Control System (Aqua Medic Company) and was settled controlling the partial pressure of CO_2. To measure the total alkalinity, samples of *P. pavonica* were placed with seawater in a glass bottle with a screw top cap and kept in the refrigerator until analysis. The measurements were carried out on samples in time 0 and after 2 h of incubation with lighting (80−100 μmol quanta s m^{-2}) using an automated Mettler-Toledo DL-67 autotitrator. The pH electrode was calibrated with buffer solutions (4, 7, and 9), and the pH readings were performed according to it. The titration was performed with concentrations of HCl, 0.2 or 0.05 M (depending upon the sample). The calibration was carried out using Dickson carbonate chemistry standards.

Sample Characterization. For the characterization of the mineral content and phase of the *P. pavonica* samples, the following procedure was adopted. Once removed from seawater, the thallus of the samples was mechanically separated by the holdfast, which was often matted. The blades were then carefully washed with deionized water and stored in ethanol.

For the X-ray powder diffraction and Fourier transform infrared (FTIR) spectroscopy analyses, the sample were air-dried and ground in a mortar with the help of liquid N_2. The obtained powder was then used without any further treatment. The mineral phase was not separated by the biopolymeric matrix.

X-ray powder diffraction patterns of the samples were collected using a PanAnalytical X'Pert Pro equipped with an X'Celerator detector powder diffractometer using Cu Kα radiation generated at 40 kV and 40 mA. The diffraction patterns were collected within the 2θ range from 5° to 70° with a step size ($\Delta 2\theta$) of 0.02° and a counting time of 300 s. The samples were loaded on a low background silica holder. The X-ray powder diffraction patterns were analyzed using the X'Pert HighScore Plus software (PANalytical). A quantitative analysis of the crystalline phases was performed using the software "Quanto" (see http://www.ba.ic.cnr.it/softwareic/), which is based on the Rietveld method.[27] The following mineral phases were considered: aragonite, magnesium calcite, gypsum, bassanite, and anhydrite. During the refinement process, correction for preferential orientation was applied, when

DOI: 10.1021/acsearthspacechem.7b00051
ACS Earth Space Chem. XXXX, XXX, XXX−XXX

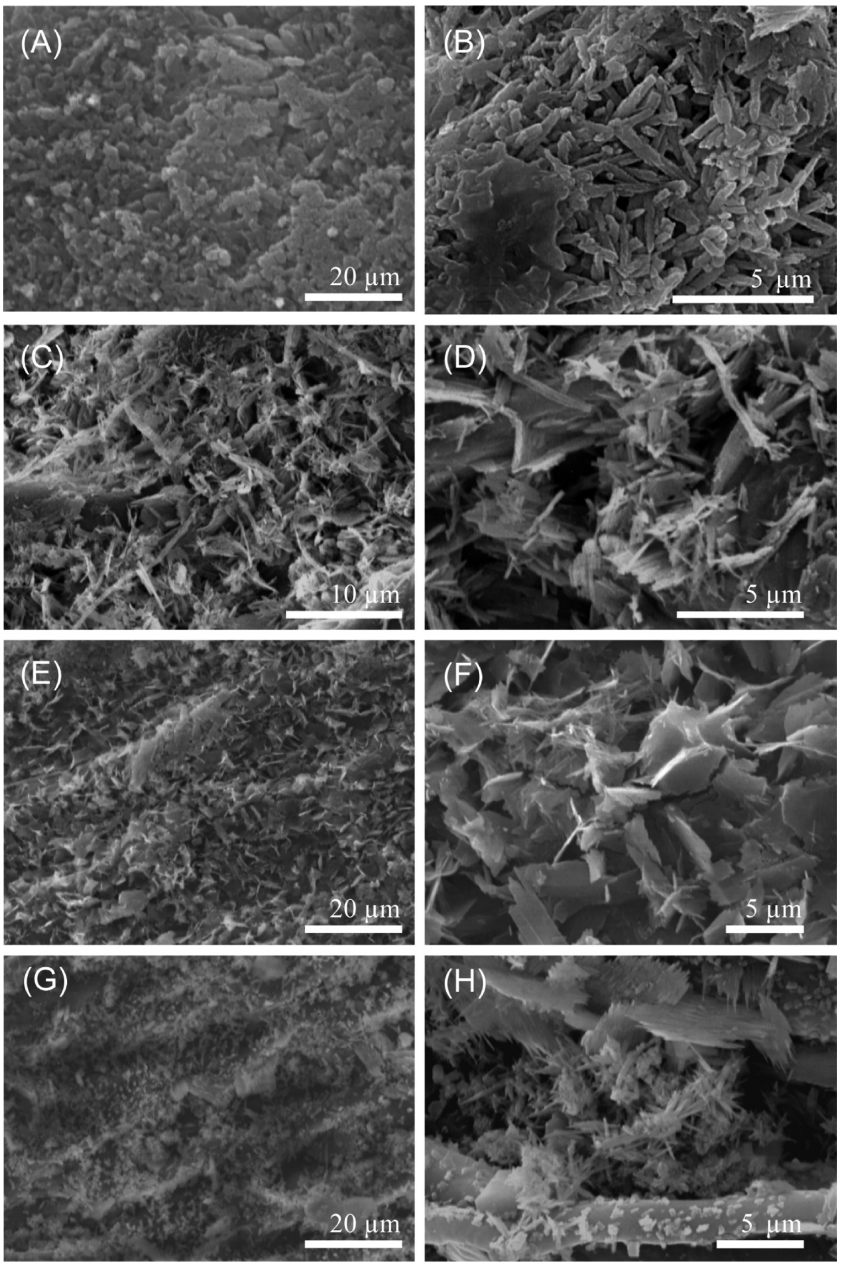

Figure 3. SEM pictures of *P. pavonica* samples collected at the CO_2 vent: (A and B) sample collected in Site 1 at pH_{TS} 8.1, (C and D) sample collected in Site 4 at pH_{TS} 7.4, (E and F) sample collected in Site 1 at pH_{TS} 8.1 and transplanted to Site 4 at pH_{TS} 7.4 for 7 days, and (G and H) sample collected in Site 4 at pH_{TS} 7.4 and transplanted to Site 1 at pH_{TS} 8.1 for 7 days. Each image is the most representative of the whole sample and shows one of the most calcified regions.

necessary. The refinement process was considered complete when the GoF factor (a figure of merit) was below 5.[27]

A low amount (around 5 mg) of powder samples was analyzed by means of FTIR spectroscopy analyses conducted using a FTIR Nicolet 380, Thermo Electron Corporation, working in the range of wavenumbers of 400−4000 cm^{-1} at a resolution of 2 cm^{-1}. A disk was obtained mixing a small amount (<1 mg) of sample with 100 mg of KBr and applying a pressure of 48.6 tsi (670.2 MPa) to the mixture using a hydraulic press.

An estimation of the organic matter content in the sample was determined by thermogravimetric analysis (TGA) on a SDT Q600 simultaneous thermal analysis instrument (TA Instruments). Pieces from the central region of the thallus having a weight of about 10 mg were used. The analysis was performed under nitrogen flow from 30 to 120 °C with a heating rate of 10 °C min^{-1}, an isothermal at 120 °C for 5 min, and another cycle from 120 to 600 °C with the same heating rate. The reported values are the average of at least three independent measurements.

The optical microscope observations of samples were made with a Leica microscope equipped with a digital camera. The scanning electron microscopy (SEM) observations were conducted in a Phenom microscope (FEI) for uncoated samples and a Hitachi FEG 6400 microscope for samples following gold coating. The crystals were identified according to their morphology. Presented images are representative of the entire population of each sample.

DOI: 10.1021/acsearthspacechem.7b00051
ACS Earth Space Chem. XXXX, XXX, XXX−XXX

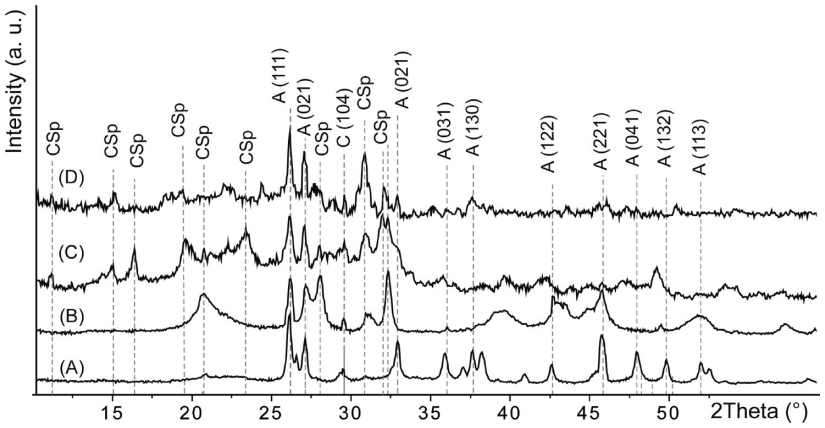

Figure 4. X-ray powder diffraction pattern of samples of *P. pavonica* collected at the CO_2 vent and kept in aquaria: (A) sample collected in Site 1 and kept in aquaria for 7 days at pH_{TS} 8.1, (B) sample kept in aquaria for 7 days at pH_{TS} 8.1 and then transplanted in aquaria at pH_{TS} 7.4 for 7 days, (C) sample collected in Site 4 and kept in aquaria for 7 days at pH_{TS} 7.4, and (D) sample kept in aquaria for 7 days at pH_{TS} 7.4 and then transplanted in aquaria at pH_{TS} 8.1 for 7 days. A, C, and CSp indicate aragonite, magnesium calcite, and calcium sulfate phases, respectively. The Miller indexes of aragonite diffraction peaks are indicated.

RESULTS

Samples of *P. pavonica* transplanted along the gradient showed a reduction of the calcified regions moving from pH_{TS} 8.1 to 7.4. This could be seen by the naked eye by the degree of mineral coverage of the thallus (Figure 1) and was quantified from 71 ± 3 to 60 ± 4 wt % mineral percentage of dry thallus (Table 1) by thermogravimetrical analysis. The diffractometric (Figure 2) and spectroscopic (Figure SI1 of the Supporting Information) analyses showed also that the mineral composition changed. The amount of aragonite was reduced from 97 ± 2 to 21 ± 3 wt % in favor of calcium sulfate phases and a minor amount of magnesium calcite (Table 1). A mixture of calcium sulfate phases having a diverse hydration status was detected, with the main calcium sulfate phases being gypsum, bassanite, and anhydrite. The presence of anhydrite was particularly puzzling because anhydrite does not form at a low temperature.[28] Thus, the formation of anhydrite could be due to a dehydration process of hydrated calcium sulfate phases associated with the storage and handling of the samples. For this reason, the content of calcium sulfate phases is reported as a whole. When the native samples were transplanted from pH_{TS} 7.4 to 8.1, only a small increase of the mineral coverage (Figure 2) was observed as the percentage of mineral (Table 1) increased from 61 ± 2 to 66 ± 3 wt %. The mineralogy of the thalli (Figure 2 and Figure SI1 of the Supporting Information) showed that the percentage of aragonite increased from 21 ± 5 to 39 ± 4 wt %, while the percentage of calcium sulfate phases decreased from 75 ± 11 to 57 ± 6 wt %. The SEM pictures showed the mineral morphology (Figure 3). Aragonite appeared as needles, while the calcium sulfate phases had tablet-like shapes, regardless of pH_{TS}.

Samples collected from sites 1 and 4 (pH_{TS} 8.1 and 7.4) at Panarea and kept in aquaria (acclimated) at pH_{TS} 8.1 and 7.4, respectively, did not change in mineral coverage, content, or composition (Figures 4 and 5, Figure SI2 of the Supporting Information, and Table 1). Samples acclimated at pH_{TS} 8.1 and kept for 1 week in aquaria at pH_{TS} 7.4 decalcified (Figure 4 and Table 1), reduced the mineral percentage from 71 ± 3 to 60 ± 5 wt %, reduced the percentage of aragonite from 97 ± 2 to 62 ± 7 wt % (Figure 4, Figure SI2 of the Supporting Information, and Table 1), and increased the calcium sulfate phases from 1 ± 0.5 to 38 ± 5 wt %. Samples acclimated at (pH_{TS} 7.4) and kept in aquaria for 1 week at pH_{TS} 8.1 showed a slight increase of the mineral percentage of the algae from 62 ± 3 to 68 ± 3 wt %, an increase of aragonite from 26 ± 4 to 38 ± 5 wt %, and a decrease of the calcium sulfate phases from 72 ± 10 to 60 ± 10 wt %. SEM of the samples kept in aquaria (Figure 5) showed the presence of aragonite needles and calcium sulfate phases having tablet-like shapes independent from the sample treatment.

DISCUSSION

The submarine CO_2 vent off Panarea Island, previously characterized from a geochemical point of view,[29] acidifies the surrounding seawater affecting different native species, such as *P. pavonica*, who decalcifies with increasing acidity.[10] This result is in agreement with previous studies, where aragonitic corals, calcareous algae, and epibionts were observed to lose $CaCO_3$ under acidified conditions.[10−12,26,30−32] The present study suggests that *P. pavonica* is sensitive to pH variations but also resilient, because the alga not only thrived at the low pH site but also partially recovered initial $CaCO_3$ loss once returned to normal pH conditions. In addition, because a lack of correlation between photosynthesis and carbonate deposition in three species from the genus *Padina* (among them *P. pavonica*) was previously observed,[33] calcification may not be directly related to the photosynthetic efficiency, as also recently reported in the case of some coral sites.[34] Studies have already shown that this alga adapts its physiological performance in hypercapnic/acidic environments, behaving as a sun-adapted species instead of a shade-adapted species as a response to the lower calcium carbonate coverage and, thus, to increased exposure to solar radiation.[35,36] In general, it is expected that, as the acidity induces reduction of the highly reflective and opaque calcified cover, the exposure of *P. pavonica* thalli to high light dramatically increases compared to its calcified status. It is plausible that the dominance of *P. pavonica* in shallow waters, high irradiance sites, stems from its calcified cover. It is noteworthy that *Padina* is among the very few brown algae that both calcify and are successful under high light, suggesting a causal link among these features. Johnson et al. in Papua New Guinea observed that, in shallow, clear, high pCO_2 waters, the abundance of lightly calcified *Padina* spp. increased. This was explained suggesting a reduced sea urchin grazing pressure and

DOI: 10.1021/acsearthspacechem.7b00051
ACS Earth Space Chem. XXXX, XXX, XXX−XXX

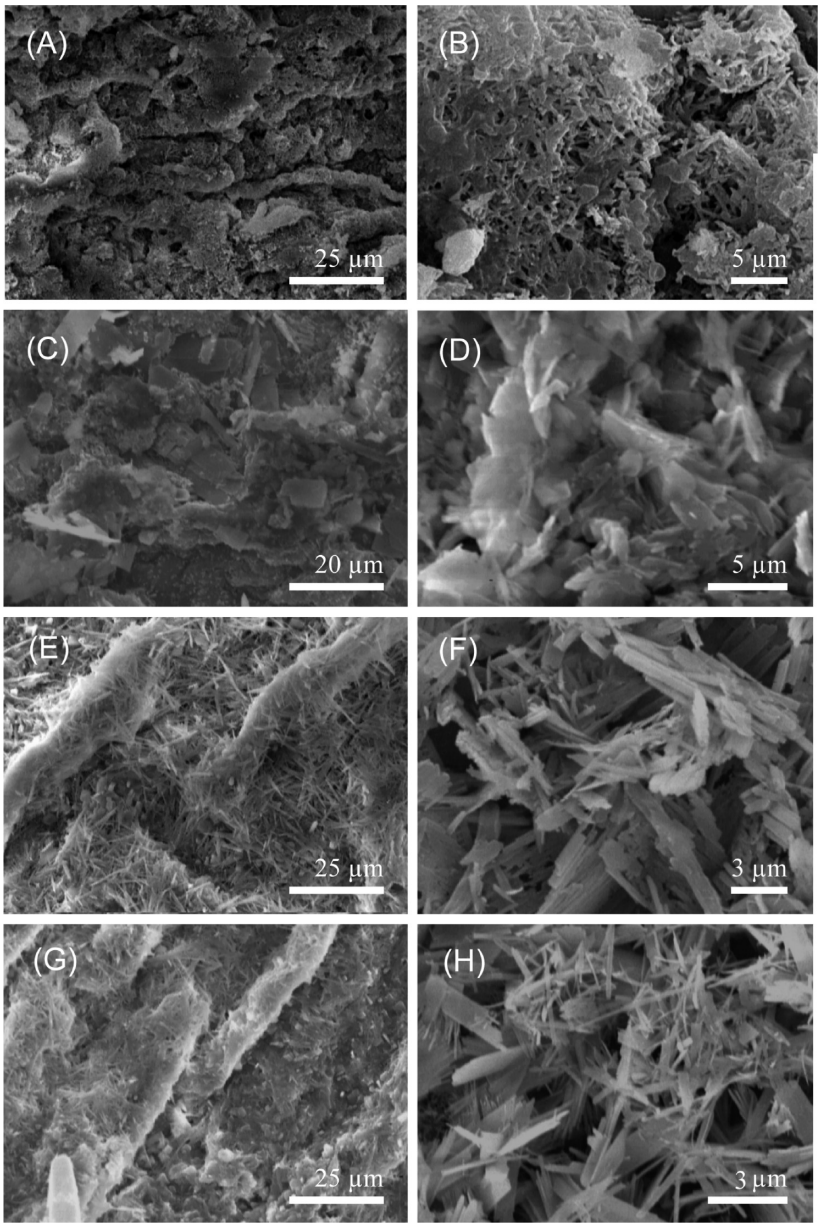

Figure 5. SEM pictures of samples of *P. pavonica* collected at the CO_2 vent and kept in aquaria: (A and B) sample collected in Site 1 and kept in aquaria for 7 days at pH_{TS} 8.1, (C and D) sample kept in aquaria for 7 days at pH_{TS} 8.1 and then transplanted in aquaria at pH_{TS} 7.4 for 7 days, (E and F) sample collected in Site 4 and kept in aquaria for 7 days at pH_{TS} 7.4, and (G and H) sample kept in aquaria for 7 days at pH_{TS} 7.4 and then transplanted in aquaria at pH_{TS} 8.1 for 7 days. The images were taken on the thallus side exposed to light, which is the most calcified. Each image is the most representative of the whole sample and shows one of the most calcified regions.

significant increases in photosynthetic rates.[11] The responses of macroalgae of non-calcified macroalga *Cystoseira compressa* (Phaeophyceae, Fucales) and calcified *P. pavonica* were studied near a pCO_2 seep in oligotrophic waters. It was shown that both algae benefitted from elevated pCO_2 levels, although their responses varied depending upon light and nutrient availability.[37]

OA is likely to wipe out that competitive advantage and exclude the species from such sites. This suggests a thriving capacity under OA conditions,[38] however, limited to relatively shaded or deeper sites. *P. pavonica* under low pH was subject to decalcification and to a change in the mineralogy of calcification in favor of hydrated calcium sulfate salts, as previously reported.[10] The presence of CO_2 leads to a reduction of the aragonite saturation state, which promotes its dissolution. A concomitant precipitation of calcium sulfate phase is observed. The local increase of the calcium ion concentration as a result of aragonite dissolution may favor the observed precipitation of calcium sulfate phases because the seawater solution contains sulfate ions. This may occur through a secondary mineral precipitation process.[39,40] Nevertheless, seawater is undersaturated with respect to bassanite and slightly undersaturated with respect to gypsum. Thus, a stabilization of the calcium sulfate mineral phases by *P. pavonica* superficial and/or released macromolecules may be hypostasized. The possibility that the precipitation of calcium sulfate phases occurred as a consequence of the sample storage in ethanol[41] appears highly improbable because (i) the samples were carefully washed with deionized water before their storage and (ii) another algal species, *A. acetabulum*, which had the same handling and

DOI: 10.1021/acsearthspacechem.7b00051
ACS Earth Space Chem. XXXX, XXX, XXX−XXX

storage process before the characterization, did not show the presence of calcium sulfate phases.[10]

This research confirms that natural "laboratories", such as submarine CO_2 vents, are considered invaluable environments that provide the closest insight into what might happen in the future, especially when other parameters (e.g., seawater temperature and nutrients) are unaffected.[42,43] However, such parameters cannot be controlled as in experiments conducted under controlled conditions in aquaria. Thus, the fact that, in the present study, the effects observed around the submarine CO_2 vent were consistent with those observed in aquaria strengthens the results obtained in the field, at least for short-term responses (7 days).

It is important to note that the pH values around the CO_2 vent and in aquaria surpass the most pessimistic scenarios of global ocean surface pH predicted for the end of the century (i.e., between 0.30 and 0.32 for the Representative Concentration Pathway 8.5)[1] and, thus, may give insights on possible responses to even further OA scenarios. However, the implications of changes in *Padina* spp. biomineralization on mechanical strength, dissolution rates, bicarbonate and nutrient assimilation through the generation of protons, photosynthetic performance overall protection from excess irradiance, and grazer deterrence need further investigation.

In conclusion, because *P. pavonica* is a sensitive reporter of acute environmental pH changes, this suggests that *P. pavonica* could be a suitable bioindicator of OA. New research could provide insights on how this calcifying macroalgae behaves seasonally and under future OA conditions by combining regular *in situ* image (non-destructive optical reflectance) monitoring of calcium carbonate deposition coupled to continuous physical−chemical measurements.

Furthermore, studies are needed to investigate the effects of OA on additional macroalgae and their grazers, because these underpin the ecology of rocky shores. An exclusion experiment was used to test effects of herbivory in benthic communities along a pCO_2 gradient. Sea urchins and herbivorous fish dramatically reduced macroalgal biomass at background carbon dioxide levels; this effect was not hampered by increased pCO_2, despite lower sea urchin densities near the seeps, because herbivorous fish abundances increased concurrently.[44]

Given the extensive distribution of this species, replicated observations are required across multiple regions, resulting in a wider geographic range monitoring program to increase confidence in predictions of the ecological impacts of OA on a global scale.

■ ASSOCIATED CONTENT

Supporting Information

The Supporting Information is available free of charge on the ACS Publications website at DOI: 10.1021/acsearthspacechem.7b00051.

Spectroscopic analyses of *P. pavonica* samples by means of FTIR spectroscopy (PDF)

■ AUTHOR INFORMATION

Corresponding Author

*E-mail: giuseppe.falini@unibo.it.

ORCID

Giuseppe Falini: 0000-0002-2367-3721

Notes

The authors declare no competing financial interest.

■ ACKNOWLEDGMENTS

The research leading to these results has received funding from the European Research Council under the European Union's Seventh Framework Programme (FP7/2007-2013)/ERC grant agreement n8 [249930- CoralWarm: Corals and global warming: the Mediterranean versus the Red Sea]. Giuseppe Falini and Simona Fermani thank the Consorzio Interuniversitario per la Chimica dei Metalli nei Sistemi Biologici for the support.

■ REFERENCES

(1) Hoegh-Guldberg, O.; Cai, R.; Poloczanska, E. S.; Brewer, P. G.; Sundby, S.; et al. The Ocean. In *Climate Change 2014: Impacts, Adaptation, and Vulnerability. Part B: Regional Aspects. Contribution of Working Group II to the Fifth Assessment Report of the Intergovernmental Panel of Climate Change*; Barros, V. R., Field, C. B., Dokken, D. J., Mastrandrea, M. D., Mach, K. J., et al., Eds.; Cambridge University Press: New York, 2014; pp 1655−1731.

(2) Gattuso, J.-P.; Magnan, A.; Billé, R.; Cheung, W.; Howes, E.; et al. Contrasting futures for ocean and society from different anthropogenic CO_2 emissions scenarios. *Science* **2015**, *349*, aac4722.

(3) Arèvalo, R.; Pinedo, S.; Ballesteros, E. Changes in the composition and structure of Mediterranean rocky-shore communities following a gradient of nutrient enrichment: Descriptive study and test of proposed methods to assess water quality regarding macroalgae. *Mar. Pollut. Bull.* **2007**, *55*, 104−113.

(4) Juanes, J. A.; Guinda, X.; Puente, A.; Revilla, J. A. Macroalgae, a suitable indicator of the ecological status of coastal rocky communities in the NE Atlantic. *Ecol. Indic.* **2008**, *8*, 351−359.

(5) Abbot, I. A.; Huisman, J. M. New species, observations, and a list of new records of brown algae (Phaeophyceae) from the Hawaiian Islands. *Phycol. Res.* **2003**, *51*, 173−185.

(6) Silberfeld, T.; Bittner, L.; Fernàndez-Garcìa, C.; Cruaud, C.; Rousseau, F.; et al. Species diversity, phylogeny and large scale biogeographic patterns of the genus *Padina* (Phaeophyceae, Dictyotales). *J. Phycol.* **2013**, *49*, 130−142.

(7) Guiry, M. D. *Algaebase*; World-Wide Electronic Publication, National University of Ireland: Galway, Ireland, 2010; http://www.algaebase.org.

(8) Lüning, K.; Dring, M. J. Action spectra and spectral quantum yield of photosynthesis in marine macroalgae with thin and thick thalli. *Mar. Biol.* **1985**, *87*, 119−129.

(9) Lowenstam, H. A.; Weiner, S. *On Biomineralization*; Oxford University Press: New York, 1989.

(10) Goffredo, S.; Prada, F.; Caroselli, E.; Pasquini, L.; Fantazzini, P.; et al. Biomineralization control related to population density under ocean acidification. *Nat. Clim. Change* **2014**, *4*, 593−597.

(11) Johnson, V. R.; Russell, B. D.; Fabricius, K. E.; Brownlee, C.; Hall-Spencer, J. M. Temperate and tropical brown macroalgae thrive, despite decalcification, along natural CO_2 gradients. *Glob. Change Biol.* **2012**, *18*, 2792−2803.

(12) Okazaki, M.; Pentecost, A.; Tanaka, Y.; Miyata, M. A study of calcium carbonate deposition in the genus *Padina* (Phaeophyceae, Dictyotales). *Br. Phycol. J.* **1986**, *21*, 217−224.

(13) Borowitzka, M. A.; Larkum, A.W. D.; Nockolds, C. D. A scanning microscope study of the structure and organization of the calcium carbonate deposits of algae. *Phycologia* **1974**, *13*, 195−203.

(14) Bürger, K.; Clifford, E. L.; Schagerl, M. Morphological changes with depth in the calcareous brown alga *Padina pavonica*. *Bot. Mar.* **2017**, *60*, 171−180.

(15) Wynne, M. J.; de Clerck, O. First reports of *Padina antillarum* and *P. glabra* (Phaeophyta-Dictyotaceae) from Florida, with a Key to the Western Atlantic Species of the Genus. *Caribb. J. Sci.* **1999**, *35*, 286−295.

(16) Borowitzka, M. A.; Larkum, A. W. D. Calcification in the green alga *Halimeda*. II. The exchange of Ca^{2+} and the occurrence of age

DOI: 10.1021/acsearthspacechem.7b00051
ACS Earth Space Chem. XXXX, XXX, XXX−XXX

gradients in calcification and photosynthesis. *J. Exp. Bot.* **1976**, *27*, 864−878.
(17) de Beer, D.; Larkum, A. W. D. Photosynthesis and calcification in the calcifying algae *Halimeda discoidea* studied with microsensors. *Plant, Cell Environ.* **2001**, *24*, 1209−1217.
(18) McConnaughey, T. Acid secretion, calcification, and photosynthetic carbon concentrating mechanisms. *Can. J. Bot.* **1998**, *76*, 1119−1126.
(19) Sand-Jensen, K.; Gordon, D. M. Differential ability of marine and freshwater macrophytes to utilize HCO_3^- and CO_2. *Mar. Biol.* **1984**, *80*, 247−253.
(20) Bradassi, F.; Cumani, F.; Bressan, G.; Dupont, S. Early reproductive stages in the crustose coralline alga *Phymatolithon lenormandii* are strongly affected by mild ocean acidification. *Mar. Biol.* **2013**, *60*, 2261−2269.
(21) Newcomb, L. A.; Milazzo, M.; Hall-Spencer, J. M.; Carrington, E. Ocean acidification bends the mermaid's wineglass. *Biol. Lett.* **2015**, *11*, 20141075.
(22) McConnaughey, A. T.; Whelan, J. F. Calcification generates protons for nutrient and bicarbonate uptake. *Earth-Sci. Rev.* **1997**, *42*, 95−17.
(23) Littler, M. M.; Littler, D. S. The evolution of thallus form and survival strategies in benthic marine macroalgae: Field and laboratory tests of a functional form model. *Am. Nat.* **1980**, *116*, 25−44.
(24) Padilla, D. K. Rip-stop in marine algae: Minimising the consequences of herbivore damage. *Evol. Ecol.* **1993**, *7*, 634−644.
(25) Pettit, L. R.; Smart, C. W.; Hart, M. B.; Milazzo, M.; Hall-Spencer, J. M. Seaweed fails to prevent ocean acidification impact on foraminifera along a shallow-water CO_2 gradient. *Ecol. Evol.* **2015**, *5*, 1784−1793.
(26) Gil-Díaz, T.; Haroun, R.; Tuya, F.; Betancor, S.; Viera-Rodríguez, M. A. Effects of Ocean Acidification on the Brown Alga *Padina pavonica*: Decalcification Due to Acute and Chronic Events. *PLoS One* **2014**, *9*, e108630.
(27) Altomare, A.; Burla, M. C.; Giacovazzo, C.; Guagliardi, A.; Moliterni, A. G. G.; Polidori, G.; Rizzi, R. Quanto: A Rietveld program for quantitative phase analysis of polycrystalline mixtures. *J. Appl. Crystallogr.* **2001**, *34*, 392−397.
(28) Ossorio, M.; Van Driessche, A. E. S.; Pérez, P.; García-Ruiz, J. M. The gypsum−anhydrite paradox revisited. *Chem. Geol.* **2014**, *386*, 16−21.
(29) Capaccioni, B.; Tassi, F.; Vaselli, O.; Tedesco, D.; Poreda, R. Submarine gas burst at Panarea Island (southern Italy) on 3 November 2002: A magmatic versus hydrothermal episode. *J. Geophys. Res.* **2007**, *112*, B05201.
(30) Orr, J. C.; Fabry, V. J.; Aumont, O.; Bopp, L.; Doney, S. C.; et al. Anthropogenic ocean acidification over the twenty-first century and its impact on calcifying organisms. *Nature* **2005**, *437*, 681−686.
(31) Kleypas, J. A.; Buddemeier, R. W.; Archer, D.; Gattuso, J.-P.; Langdon, C.; et al. Geochemical consequences of increased atmospheric carbon dioxide on coral reefs. *Science* **1999**, *284*, 118−120.
(32) Fantazzini, P.; Mengoli, S.; Pasquini, L.; Di Giosia, M.; Fermani, S.; et al. Gains and losses of coral skeletal porosity changes with ocean acidification acclimation. *Nat. Commun.* **2015**, *6*, 7785.
(33) Wefer, G. Carbonate production by algae Halimeda, Penicillus and Padina. *Nature* **1980**, *285*, 323−324.
(34) Cohen, I.; Dubinsky, Z.; Erez, J. Light Enhanced Calcification in Hermatypic Corals: New Insights from Light Spectral Responses. *Front. Mar. Sci.* **2016**, *2*, 122.
(35) Dubinsky, Z.; Falkowski, P. G.; Wyman, K. Light harvesting and utilization in phytoplankton. *Plant Cell Physiol.* **1986**, *27*, 1335−1350.
(36) Dubinsky, Z.; Schofield, O. The light from the darkness: Thriving at the light extremes in nature. *Hydrobiologia* **2010**, *639*, 153−171.
(37) Celis-Plá, P. S. M.; Hall-Spencer, J. M.; Horta, P. A.; Milazzo, M.; Korbee, N.; Cornwall, C. E.; Figueroa, F. L. Macroalgal responses to ocean acidification depend on nutrient and light levels. *Front. Mar. Sci.* **2015**, *2*, 26.
(38) Betancor, S.; Tuya, F.; Gil-Diaz, T.; Figueroa, F. L.; Haroun, R. Effects of a submarine eruption on the performance of two brown seaweeds. *J. Sea Res.* **2014**, *87*, 68−78.
(39) Garcia-Rios, M.; Cama, J.; Luquot, L.; Soler, J. M. *Chem. Geol.* **2014**, *383*, 107−122.
(40) Van Driessche, A. E. S.; Stawski, T. M.; Benning, L. A.; Kellermeier, M. Calcium sulfate precipitation throughout its phase diagram. In *New Perspectives on Mineral Nucleation and Growth: From Solution Precursors to Solid Materials*; Van Driessche, A. E. S., Kellermeier, M., Benning, L. G., Gebauer, D., Eds.; Springer: Cham, Switzerland, 2017; pp 227−254, DOI: 10.1007/978-3-319-45669-0_12.
(41) Tritschler, U.; Kellermeier, M.; Debus, C.; Kempterc, A.; Cölfen, H. A simple strategy for the synthesis of well-defined bassanite nanorods. *CrystEngComm* **2015**, *17*, 3772−3776.
(42) Hall-Spencer, J. M.; Rodolfo-Metalpa, R.; Martin, S.; Ransome, E.; Fine, M.; et al. Volcanic carbon dioxide vents show ecosystem effects of ocean acidification. *Nature* **2008**, *454*, 96−99.
(43) Fabricius, K. E.; Déath, G.; Noonan, S.; Uthicke, S. Ecological effects of ocean acidification and habitat complexity on reef-associated macroinvertebrate communities. *Proc. R. Soc. B* **2014**, *281*, 20132479.
(44) Baggini, C.; Issaris, Y.; Maria Salomidi, M.; Hall-Spencer, J. Herbivore diversity improves benthic community resilience to ocean acidification. *J. Exp. Mar. Biol. Ecol.* **2015**, *469*, 98−104.

DOI: 10.1021/acsearthspacechem.7b00051
ACS Earth Space Chem. XXXX, XXX, XXX−XXX